MODELING REACH SCALE RESPONSE TO CONTROLLED FLOWS ON THE WILLAMETTE RIVER

by

DION MARCEL WEBSTER

A THESIS

Presented to the Department of Geography
and the Division of Graduate Studies of the University of Oregon
in partial fulfillment of the requirements
for the degree of
Master of Science

September 2021

THESIS APPROVAL PAGE

Student: Dion Marcel Webster

Title: Modeling Reach Scale Response to Controlled Flows on the Willamette River

This thesis has been accepted and approved in partial fulfillment of the requirements for the Master of Science degree in the Department of Geography by:

Mark Fonstad	Chairperson
Patricia McDowell	Member

and

Andrew Karduna	Interim Vice Provost for Graduate Studies

Original approval signatures are on file with the University of Oregon Division of Graduate Studies.

Degree awarded September 2021

© 2021 Dion Marcel Webster

THESIS ABSTRACT

Dion Marcel Webster

Master of Science

Department of Geography

September 2021

Title: Modeling Reach Scale Response to Controlled Flows on the Willamette River

The upper Willamette river was historically a multi-threaded gravel-bed river. The multidecadal effects of a reduced flow regime, sediment flux, recruitment of large woody debris and bank stabilization caused by anthropogenic disturbances have resulted in decreased riverscape complexity. This project incorporates a 2D hydrodynamic landscape evolution model to simulate the extent of functional floodplain and the erosion/deposition patterns associated with the functional flow event for a segment of the upper Willamette River. The functional floodplain simulation indicated secondary features with tall banks and majority of the geomorphic change occurring in the main channel and adjacent bars rather than the floodplain features. Compared to a previous study on potential 2-year flood extent, the contemporary functional floodplain is drastically smaller. Modeling results show high precision values for inundation and a need for more erosion/deposition validation data. Results from this study also advocate for the inclusion of more landscape evolution model simulations for future restoration efforts.

CURRICULUM VITAE

NAME OF AUTHOR: Dion Marcel Webster

GRADUATE AND UNDERGRADUATE SCHOOLS ATTENDED:

University of Oregon, Eugene
Texas A&M University, College Station, Texas
Blinn College, Bryan, Texas

DEGREES AWARDED:

Master of Science, Geography, 2021 University of Oregon
Bachelor of Science, Geography, 2019 Texas A&M University
Associate of Arts, Geography, 2018 Blinn College

AREAS OF SPECIAL INTEREST:

Fluvial Geomorphology
Numerical Modeling
Ecological Restoration

PROFESSIONAL EXPERIENCE:

GIS Intern, The Freshwater Trust, May 2021 - Present

Graduate Teaching Fellow, University of Oregon, Eugene, Oregon, October 2019 – October 2020, March – June 2021

Graduate Research Assistant, University of Oregon, Eugene, Oregon, October 2020 – March 2021

GRANTS, AWARDS, AND HONORS:

William G. Loy Award for Excellence in Cartography, "The Ogallala Aquifer: Agricultural Chokehold", University of Oregon, 2020

ACKNOWLEDGMENTS

I wish to express my appreciation to Professors Mark Fonstad and Pat McDowell for their guidance and overall support. I want to thank Mark for his mentorship and the knowledge and practice of science, and I want to thank Pat for introducing restoration and the intricacies of human-environment interaction. I would like to thank Rose Wallick and James White at the USGS Portland office for providing insight used in this project. I wish to thank the U. S. Army Corps of Engineers and Quantum Spatial, Inc. for providing foundational data used in this project. I would like to thank the University of Oregon Department of Geography for their support as a community and financially. Finally, I would like the thank my family for encouraging me to keep growing in all aspects of life.

TABLE OF CONTENTS

TABLE OF CONTENTS

Chapter Page

LIST OF FIGURES

Figure Page

LIST OF TABLES

Table Page

CHAPTER I

INTRODUCTION

Understanding the functional floodplain of the Willamette River is vital to the restoration and management of river ecosystem productivity moving forward (Wallick et al, 2013). Maps have included historical data to visualize previous active channel change, but the need for contemporary measurements has long been unexplored (Gregory et al. 2002). Since the completion of flood control dams and reservoirs on the tributaries of the Willamette, high magnitude flows have been reduced and the activity of geomorphic processes has dwindled (Risley et al. 2010). Combined with other drivers such as decreased sediment transport, the removal of large woody debris, and bank stabilization; the Willamette River's channel complexity decreased over several decades. With flow being one of the main drivers in geomorphic change, flow alteration consequently impacts river ecosystems as well. Restoration initiatives have been implemented to improve ecosystems with an emphasis on environmental flows designed to increase habitat availability (Deweber and Peterson, 2020).

In 2013, a United States Geologic Survey (USGS) report on the geomorphic state of the Willamette argued for the development of a geomorphic understanding of the current fluvial processes for the Willamette (Wallick et al. 2013). The article positioned that although there is previous research on the effects of dams, vegetation removal, and bank stabilization, more research is needed to effectively address the issues noted as they pertain to the Willamette. One of the key knowledge gaps was the delineation of the current functional floodplain where fluvial processes actively shape the land. One potential method

to address this topic is through the use of reach-scale landscape evolution modeling, which relies on computation power to solve deterministic equations used to simulate natural processes such as flooding and sediment transport. This study attempts to explore the concept of the current functional floodplain and use of reach-scale landscape evolution models by aiming to answer the following questions:

What is the extent of the contemporary functional floodplain of the Willamette River?

How well does the CAESAR-Lisflood model perform in simulating hydraulic and geomorphic processes of the Willamette River?

Past fluvial dynamism has left relic landforms and many of these have become inactive or disconnected due to human impacts or natural processes. These features have large restoration potential, however the inability to visualize the current extent of geomorphic activity can undermine restoration projects. This study will improve our understanding of both restoration efforts and scientific research. Furthermore, the model produced from this study has the potential to be adapted to answer other hydraulic and geomorphic questions specific to the modelled study area on the Willamette.

CHAPTER II

BACKGROUND

Pre-Dam History

Records for the Willamette River date back to the fur traders in the 1900s, yet studies have dated the presence of indigenous people to be at least 7,000 years (Aikens, 1975). Before Euro-American colonization, indigenous people annually burned the valley floor to maintain prairies for confining game within small thickets, improving harvesting grain and other resources post-fire (Johannessen et al, 1970). While burned lands provide a source of nutrients to rivers, the riparian forest was described as an "impassible thicket," and the geomorphic influence of prescribed fires were considered marginal in the riparian forest (Johannessen et al., 1970; Gregory et al. 2019).

With the arrival of Euro-Americans in 1805, the evolution of the Willamette River has been traced through the reports of government institutions and previous thesis work (Wallick, 2004; Wallick et al, 2007). The changes that occur to the riverscape can be attributed to the shifts in economic activity. According to Wallick (2004), the Willamette valley was occupied by fur traders at the beginning of the 19th century with agriculture beginning around the 1830s (Johannessen 1975; Wallick, 2004). Early settlers avoided residing in the floodplain due to frequent flooding. In the 1850s the population grew due to economic opportunities of surplus agriculture and growing pressure from settlers, forcing the indigenous people to end prescribed fires. Along with the increase in agriculture and population came the increasing use of steamboat transportation. This in turn led to a push for more navigable channels and channel confinement became common

in the middle and lower Willamette. In the upper Willamette, channels changed so often that boaters rarely traveled the same channel for multiple years (Wallick et al., 2007). To improve navigation across the lower and middle Willamette, there was continuous removal of large woody debris with steamboats and dynamite, infilling of sloughs, and the construction of infrastructure intended to limit channel migration and increase main channel depth. While this improved passage in the lower Willamette, efforts to improve navigation above Harrisburg were abandoned for locomotion. By the 1890s, increases in riparian forest logging occurred due to the need for wood in developing towns, paper mills, and export (Sedell and Froggatt, 1984). A growing population with a demand for more arable land eventually led to more snagging and construction to limit channel migration. Downstream of the upper Willamette, settlers occasionally encroached on the floodplains and eventually abandoned farms due to frequent floods that would destroy crops and property. The United States Army Corps of Engineers (USACE) continued channel stabilization and channelization efforts on the middle and lower Willamette persisted while the upper reaches remained too dynamic. Flow regulation for improved channel stability and floodplain access was not addressed until 1938 with the initiation of the Willamette Valley Project.

Dams

Wallick (2004) mentions how the 1925 Flood Control Act implemented feasibility studies which ultimately resulted in the 1938 Willamette Valley Project for the development of flood control, navigation, irrigation, streamflow regulation, and hydropower along the river (USACE, 1969; Oregon State Planning Board, 1938). From 1942 to 1969, 13 dams were built, 11 of which were flood control dams (Wallick, 2004;

Wallick et al., 2013; Gregory et al., 2019). Over time, these dams have decreased sediment input and high magnitude flows to the Willamette River, with flows having frequencies lower than 10-years being largely eliminated (Gregory et al., 2007; Risley et al. 2012, Wallick et al., 2013).

The reduction in high flows and sediment transport has triggered a number of geomorphic and aquatic habitat changes. In concert with other channelization efforts, these regulated floods thought to be responsible for the decrease in channel complexity along with increasing main channel depth, bed armoring, and sediment coarsening (Klingeman, 1987; Wallick et al., 2013; Langston,2014; Gregory et al., 2019). These geomorphic changes have impacted wildlife and native tree species such as black cottonwood. These native trees rely on the development of channel bars to provide space for germination as well as relying onthe flow regime required to supply the proper water levels for root growth during stand initiation (Fierke & Kauffman, 2006). Regulated flows have reduced bar formation and the abrupt summer flow recessions have outpaced root development, therefore they have decreased in abundance. Within the lower reaches of the upper Willamette between Eugene, Oregon and Corvallis, Oregon, different stages of the Spring chinook life cycle rely on channel complexity for survival. Lateral connectivity to floodplains during higher flows provides access to other nutrient-rich habitats such as secondary channels, alcoves, and sloughs. Additionally, lateral connection of the main channel to floodplains serves as a salmonid refuge during large,

high-velocity flooding events. In all, the flood control dams are reducing the flow regime and consequently diminishing channel complexity and habitat.

Figure 1

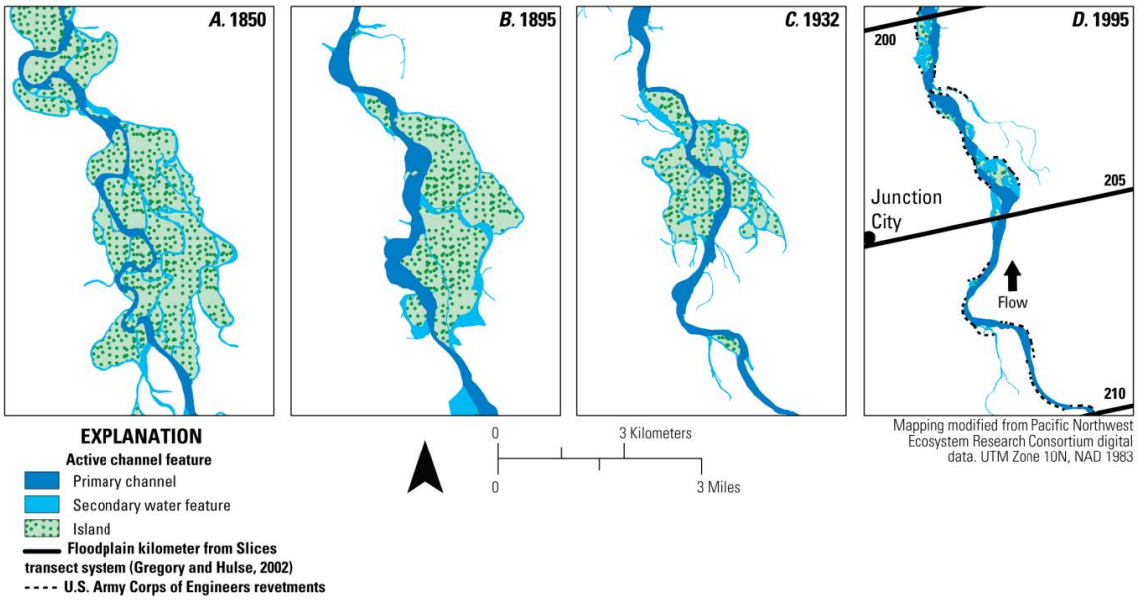

Note. (A) 1850. (B) 1895. (C) 1932. (D) 1995. figure from Wallick et al. (2013); data from Gregory et al. (2002)

Environmental Flows

In general, dams have been found to cause ecological damage and disrupt geomorphic processes along rivers (Graf, 2006; O'Connor et al., 2014). Flood control dam operations regulate the amount of discharge at a given time throughout the year resulting in the reduction of peak streamflows. Regulated releases benefit economic activities; however, these flows do not maintain pre-regulation riverine ecosystems.

Instead, reduced peak flows prevent fish passage and a multitude of other reactionary effects (Hayes et al., 2018). Environmental flows are purposeful releases from dams to provide ecological benefits; these flows aim to restore/improve riverscape ecology impacted by human derived modifications. Native plants and animals often have life stages synchronized with particular flow events which make seasonal timing and required discharge important for ecological health (Lytle & Poff, 2004; Hayes et al., 2018). Large flows that move large bedload material also produce and sustain habitats for native plants and vegetation Environmental flows include low flows, seasonal flows, pulse flows, peak flows, functional flows, and many more terms defined by geomorphic and ecological processes (Hayes et al, 2018).

This project focuses on determining the functional floodplain of a portion of the Upper Willamette River by using the term "functional flow". As described by Yarnell et al. (2015), functional flow is the component of the hydrograph that provides a geomorphic and ecological function (Escobar-Arias & Pasternack, 2010). To further elaborate on functional flow, we use the intersection between two flows defined by Hayes et al. (2018) as "habitat maintenance floods" and "channel maintenance and overbank floods." Habitat maintenance floods transport small to medium-sized sediment and increases lotic connectivity (e.g. longitudinal, lateral, vertical, and temporal) for species linked to flows (King et al., 2003; Zeug and Winemiller, 2008). Wohl (2017) refers to connectivity as "the degree to which matter (water, solutes, sediment, organic matter) and organisms can move among patches in a landscape or ecosystem" (p.347). This is a broad definition containing a subset of distinct processes each referred to by different names. In this

paper, surface water connectivity refers to flow interactions between the river and floodplain through longitudinal and lateral movement of surface water. Channel maintenance and overbank floods transport larger bedload fractions and are important drivers of channel-floodplain morphology (King et al., 2003; Opperman et al., 2010). Environmental flows attempt to improve fluvial processes and lotic connectivity by releasing prescribed streamflows during certain times of the year related to wildlife requirements such as breeding, rearing, and migration (Ward, 1989; Hays, 2018).

Previous Studies

Past studies have evaluated active channel morphology to classify the decrease in complexity and the two-year recurrence interval floodplain (Gregory et al., 2002). Gregory et al. classified the active channel throughout time and looked at the decreasing complexity of the river and side channels (Figure 1). More information is needed to understand what criteria were used to classify active channel discharge values. In 2012, River Design Group produced a two-year recurrence interval flood map using a "bathtub method" to solve flood inundation heights and extent (River Design Group Inc., 2012b). The goal of that project was to "identify restoration opportunities," i.e., identify off-channel features that could be inundated and reconnected to the main channel, using a projected stage elevation over the terrain. River Design Group modeled river stage values based on a one-dimensional model and validation data from the two flood events. The stage values were used to create an elevation gradient that would represent flooding (River Design Group Inc., 2012). The final product was a collection of potential two-year flood inundation maps. These maps show what features could potentially be inundated by a given stage, but do not verify that actual connectivity (flow into and out of) these

features exists. The final product shows what can be considered the “maximum potential of inundated area”, not necessarily the current flood extent. The maximum potential of inundated area produced by River Design Group shows a large inundated area that may be considered unrealistic. Maximum potential inundation area should be tested with sophisticated river modeling approaches that have been developed since the release of the River Design group report in 2012. This thesis will not be evaluating floodplain potential but instead look at the functional floodplain using a hydrodynamic landscape evolution model to better understand contemporary inundation and connectivity.

Figure 2

Map of the two-year regulated flow bathtub model

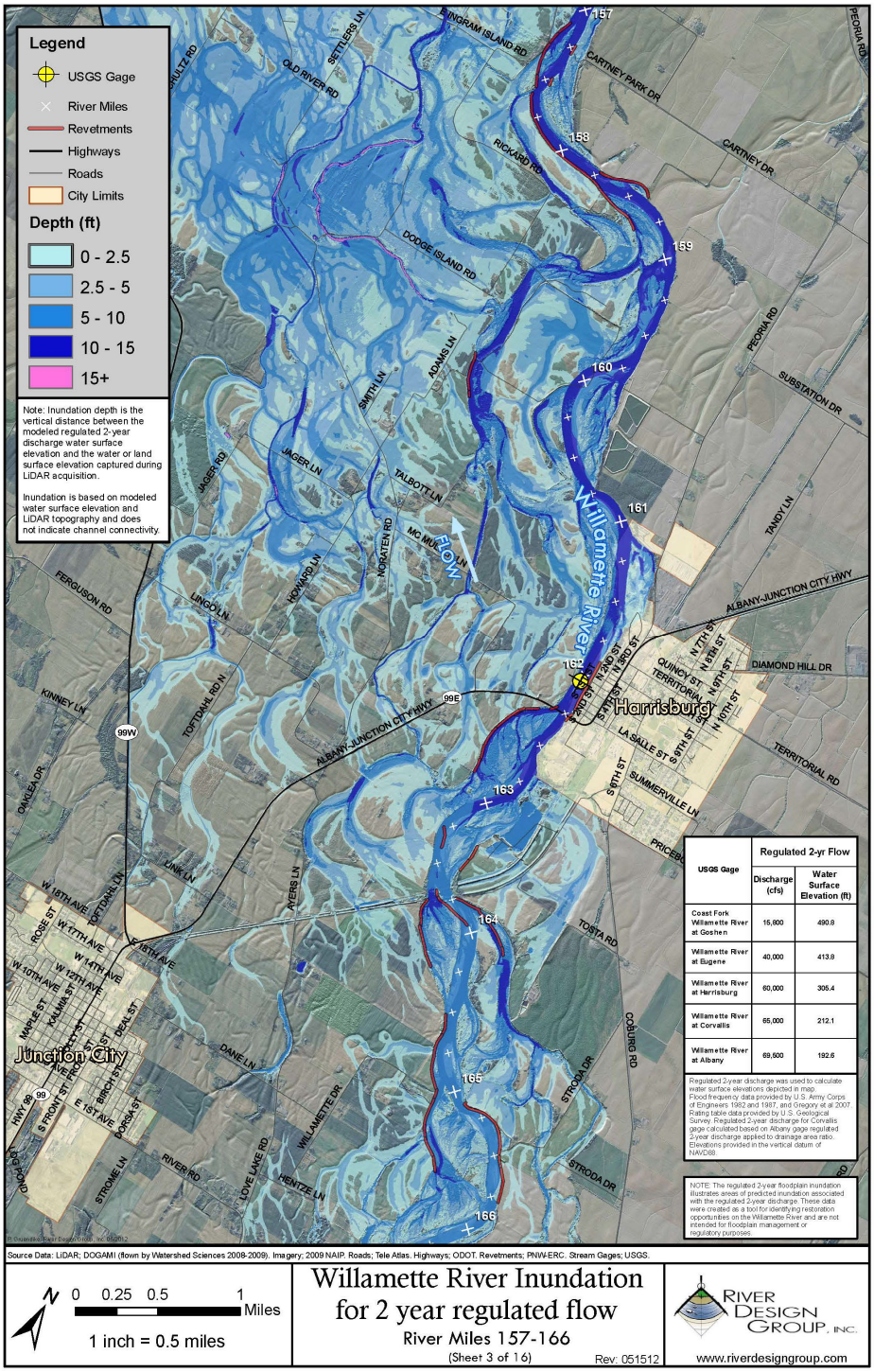

USGS Gage	Regulated 2-yr Flow	
	Discharge (cfs)	Water Surface Elevation (ft)
Coast Fork Willamette River at Goshen	15,800	490.8
Willamette River at Eugene	40,000	413.8
Willamette River at Harrisburg	60,000	305.4
Willamette River at Corvallis	65,000	212.1
Willamette River at Albany	69,500	192.6

Regulated 2-year discharge was used to calculate water surface elevations depicted in map. Flood frequency data provided by U.S. Army Corps of Engineers 1982 and 1987, and Gregory et al 2007. Rating table data provided by U.S. Geological Survey. Regulated 2-year discharge for Corvallis gage calculated based on Albany gage regulated 2-year discharge applied to drainage area ratio. Elevations provided in the vertical datum of NAVD88.

NOTE: The regulated 2-year floodplain inundation illustrates areas of predicted inundation associated with the regulated 2-year discharge. These data were created as a tool for identifying restoration opportunities on the Willamette River and are not intended for floodplain management or regulatory purposes.

Note. created by River Design Group Inc. (2012).

CHAPTER III

METHODS

Summary and Model Description

This study contains two components to determine the functional floodplain. The first component addresses surface water connectivity by utilizing the hydrodynamic 2D flow model in CAESAR-Lisflood for flood extent mapping. Observed gage data and flood extent data from the February 8th, 1996

Study site and data inputs

Data availability, riverscape complexity, and proximity to a gage determined the study reach. The reach is a 30 square-kilometer area adjacent to Junction City and Harrisburg, Oregon. This area contains low floodplain elevations and a high density of floodplain channel features (Wallick et al, 2013). As pictured in Figure 1, a terrace on the right side of the river prevents most inundation on the eastern portion of the study area while the remainder of floodplain contain a complex network of alcoves, side channels, swales, and sloughs. Previous work encompassing the study area highlights the decrease in channel complexity and dynamics (Gregory et al, 2002) and a high potential for restoration efforts (River Design Group, 2012) (Figure 2).

Figure 3

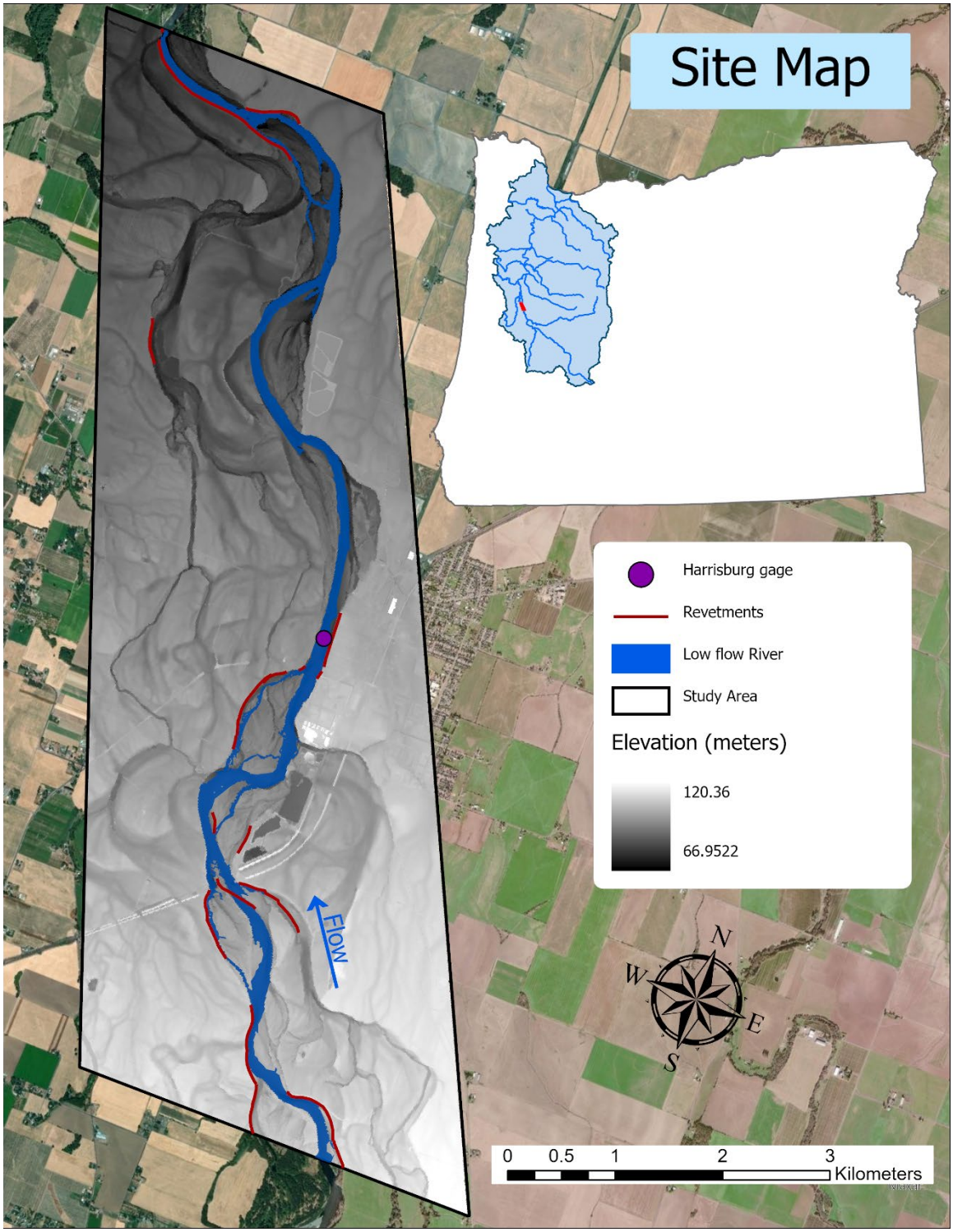
Site Map
Harrisburg gage
Revetments
Low flow River
Study Area
Elevation (meters)
120.36
66.9522
Flow
N
W
E
S
0
0.5
1
2
3
Kilometers

Functional Flow

To determine the contemporary flow associated with the functional floodplain, this project first defines the "functional floodplain." Wallick (2013) describes functional flow as "part of the river corridor actively formed and modified by fluvial processes." Previous studies have used channel bankfull flow as a representation of the functional flow and identified the $Q_{1.5}$ recurrence interval as the arbitrary value for bankfull despite not being universally accurate (Williams, 1978; Leopold,1996; Hayes, 2018). Here we use Q_n to represent the probable return period for a particular discharge where n represents the number of years. This study defines the functional floodplain based on the annual flood or $Q_{2.33}$ recurrence interval. By using $Q_{2.33}$, the functional floodplain is defined by a temporal measure rather than a geomorphic definition subject to user interpretation of channel and floodplain definitions.

Streamflow data from the National Water Information System (NWIS) web interface for the Harrisburg gage (14166000) provided annual peak flow discharges for running historical data for simulations and producing the flood frequency analysis (Equation 8).

$$R = (n + 1)/m$$

Where *R* is the recurrence interval, *n* is the number of recorded events and *m* is the particular event's rank juxtaposed to the magnitude of the other recorded events. Furthermore, the range of Harrisburg gage discharge observations spans from 1945-present, but only post dam construction years (1970-2019) were isolated to determine the contemporary functional flow. Previous studies have used the log-Pearson type III

distribution statistical fitting technique to identify large magnitude low-frequency events such as the 0.1 probability event. Given ease of use, I used the Log-normal distribution fitting technique. Previous studies (Oregon Water Resources Department and U.S. Army Corps of Engineers, 1998; River Design Group, 2012; Wallick, 2013; Langston, 2015) identified the dam construction period as the 1940s to late 1960s and use either 1968 (River Design Group, 2012b) or 1970 (Langston) as the first regulated flow starting date; this study used 1970. Recurrence intervals and discharge values were calculated for the regulation and pre-dam period separately for comparison, but only the regulated functional flow and 1996 flood event were simulated (***Table 1***). An annual peak streamflow range spanning 49 years (1970-2019) produced a $Q_{2.33}$ value of 1522.76 cms. The 1996 peak discharge was 2155 cms with a recurrence interval of 8 years. For simplicity, the hydrograph for the functional flow was represented by a proxy event from historical peak streamflow observation with similar discharge values. The 2015 water year peak streamflow served as the proxy event since the peak discharge was 1503 cms.

Table 1

Changes in flow recurrence intervals based on separate frequency analysis for the pre-dam peak stream flows and the regulated peak stream flows.

Event	Discharge at Harrisburg gage (cms)	Pre-dam recurrence interval (years)	Regulated recurrence interval (years)
Simulated functional flow	1522.76	1.22	2.33
1996 flood event	2154.91	1.93	8.17

Terrain Data

The main source of elevation data is a 2017 topo-bathymetric lidar digital elevation model (DEM) raster produced by Quantum Spatial, Inc (Quantum Spatial Inc., 2017). This 1-meter resolution raster contained missing data at the lowest depths for the main channel bathymetry. Merging the raster with supplemental sonar data gathered in 2018 by the USGS produces bathymetric depths based on raster and sonar zonal statistics (White et al. 2019). I extracted main channel cells and converted to points in ArcGIS Pro. I then merged the new points with the sonar data before converting back into raster format through nearest-neighbor interpolation. Afterward, I merged the new channel raster with the original topo-bathymetric lidar before using the fill function on the remaining holes in the floodplain (Figure 4). Conceptually, the in-channel erosion feature provided by CAESAR-Lisfood will alter the channel bottom to represent a natural shape. I further DEM adjustments by manually identifying and removing non-channel artifacts such as bridges by lowering the raster value to match the surrounding channel values. At this stage, I conducted raster resolution tests in CAESAR-Lisflood to gauge model speed. Coulthard et al. (2013) displayed that model run time increases exponentially as the number of pixels increases, leading to computational speed trials for 5-, 10-, and 20-meter resolution rasters. The 5-meter resolution raster proved to be too computationally intensive and the 20-meter raster lacked the spatial detail for floodplain features such as side channels and sloughs. The 10-meter resolution captured adequate amounts of detail and feasible simulation speed. I created a second DEM to represent revetments as well as limit erosion to 1.5 meters or less to prevent excessive erosion in particular cells. This process consisted of creating a copy of the final DEM, extracting pixels that align with a

1999 revetment layer produced by Ashkenas (2001), subtracting 1.5 meters from the DEM copy, then combining the extracted revetment pixels and the lowered DEM copy.

Sediment Data

Langston's thesis provides bedload grain size class measurements covering a large area of the main stem Willamette (Langston, 2014). Six surface grain size measurements sites along the main stem Willamette River from that 2014 study coincide with the study area for model simulations. The 2014 study conducted pebble counts on the point bar exposed at low flows recording two measurements every 0.3-meter increment for 30 meters at the centroid of point bars, parallel to the bar's longitudinal axis. After Langston averaged 200 observations per site, his study reported the average D_{16}, D_{50} and D_{84} grain size percentiles per site. Using this data, I averaged the six locations that correspond to the study site by the three grain size class values to produce D_{16}, D_{50}, and D_{84} values of 20.38 mm, 34.23mm, and 53.8mm, respectively. Lastly, the grain size total volume proportions in the model spin up reflect the class percentile.

Model Calibration and Spin-up

Model parameterization follows guidelines from the CAESAR-Lisflood website. (**Table 2**) (Caesar-Lisflood, 2019). I calibrated the model hydraulics by conducting the Monte Carlo approach for a range of Manning's n values for the 1996 flood event, then compared using the goodness-of-fit statistic described in Bates & De Roo (2000). When observed inundation extent data is available, a simple measure for model precision is comparing the flood extent of an observed flood event with a simulation of the flood

event. Using simple Boolean math, Bates and De Roo describe equation 8 as a measure that penalizes over- and underprediction of inundated areas.

$$\text{Fit}(\%) = \frac{\text{observed} \cap \text{simulated}}{\text{observed} \cup \text{simulated}} \times 100 \quad (8)$$

In this equation, *observed* represents the area extent of the observed inundation, and *simulated* represents the model output. By multiplying the fraction by 100, a percentage value is produced in which 100% represents a complete match of area.

USACE captured imagery the day after the peak discharge that I manually georeferenced with 2020 NAIP (National Agriculture Imagery Program) imagery and the 1-meter resolution topobathymetric lidar. This flood imagery served as the template for the observed inundation extent that was manually digitized and converted to a 10-meter resolution raster with identical dimensions as the model raster. Model hydraulics calibration relies on the raster functions provided by ArcGIS Pro to intersect and union the observed and modeled flood extent. Lastly, pixel count summations for pixels classified as inundated produce fit statistics for all Mannings-n value iteration simulations.

Table 2

Sediment, vegetation, and flow model parameters.

Parameter (units)	Operation	Impact and sensitivity	Parameter value selection
Sediment entrainment, transport and redistribution			
Sediment transport equation	Calculates volume of sediment eroded from a cell in a single iteration	Transport rates can vary significantly between the two formulae: Einstein (1950) and Wilcock and Crowe (2003)	Wilcock and Crowe (2003)
v_f (m s^{-1})	Suspended sediment settling velocity	Lower values increase suspended sediment deposition	Estimated using Stokes' law
ΔZ_{max} (m)	Maximum allowable elevation change per cell per iteration	Lower values restrict timestep and enhance model stability	Default = 0.02 used; can be lower for fine-resolution DEMs (10 m)
L_h (m)	Stratum thickness within the active layer system	Low values could affect transport rates through detachment limitation	Must be at least four times ΔZ_{max}. 0.01 used
N_{smooth}	Number of passes made by edge-smoothing filter that is used to calculate radius of curvature	Low values may cause irregular lateral development; high values may lead to over-smoothed channels	Low values for high-sinuosity meandering or braided systems; higher for low-sinuosity systems. Must be an integer. Estimated using meander wavelength (in grid cells)
N_{shift}	Determines number of cells the cross-channel gradient shifts downstream to model downstream bend migration	May lead to unrealistic evolution of meander bends if set incorrectly	One-tenth of N_{smooth} and must be an integer
ΔC_{max}	Calculates cross-channel gradient from radius of curvature which is used to control lateral transfer of eroded sediment from the outer to inner banks	Lower values ensure distribution across the entire channel width, but increase model run time. Higher values encourage mid-channel deposition	Default = 0.0001 used; can be increased or decreased by an order of magnitude depending on channel width or if modeling mid-channel deposition
Vegetation			
τ_{crveg} (Nm^{-2})	Threshold bed shear stress for vegetation removal by flows	Higher values relate to greater resistance to removal	Default = 20 used for model simplicity
T_{veg} (years)	Time required for vegetation to reach full maturity	Higher values negate the role of this over short timescales	Set to 1 for all cover and the "Grass now" function was initiated at 265 cms every run.
Proportion of erosion allowable at full maturity	Determines how vegetation maturity affects erosion	0–1 scale: 1 means vegetation has no impact on erosion; 0 means no erosion occurs at full maturity	For grass cover: 0.2 For forest cover: 0.1

Table 2 (continued)

Parameter (units)	Operation	Impact and sensitivity	Parameter value selection
Hydrology and flow routing			
Q_{min} (m^3 s^{-1})	Run-time optimization. Minimum discharge in a cell necessary for depth to be calculated	Higher values reduce run times but may restrict flow and erosion in peripheral cells if too high	0. 1 m
d_{min} (m)	Run-time optimization. Minimum water depth in a cell necessary for erosion to be calculated	Higher values reduce run times but may restrict flow and erosion in peripheral cells if too high	Default = 0.01 used. Can be lowered for grid cells <5m or increased for cells >50m
Q_{diff} (m^3 s^{-1})	Run-time optimization. Difference between the input and expected output discharge that can allow the model to shift to steady-state mode	Higher values reduce run times, but if too high can cause too many discharge events to be missed and lead to numerical instabilities	Can be approximated by catchment mean annual flow. User judgement also necessary regarding acceptable difference between input and output discharge and speed of model operation
h_{flow} threshold (m)	Run-time optimization. Depth through which water can flow between two cells	Higher values reduce run times but may limit flow when gradient between neighboring cells is low	Default = 0.001 used
Courant number	Controls model timestep and affects stability	Higher values increase timestep but increase risk of instabilities such as chequerboarding (rapid flow reversals between cells)	Must be 0.3–0.7. 0.4 chosen as this is recommended for 10m cells; coarser grids can use larger values
Froude number	Controls model stability and flow rate between cells	Low values reduce speed of flood waves and erosion. High values may induce chequerboarding	Default = 0.8 used. Lower values could be used for very deep, slow flows
Manning's *n*	Calculation of flow depth and velocity	High values increase flow depths, reduce flow velocities and reduce erosion	Initial estimates were chosen from reference table (Chow, 1959) and calibrated to .024 using goodness of fit (Bates & De Roo, 2000)
Slope for edge cells	Calculates flow out of the model at the downstream boundary	High values can cause excessive bed scour and upstream-propagating knickpoints; low values can cause excessive deposition at the outlet	Mean bed slope of the channel near the DEM Outlet Default = 0.001

Note. Modified from Table 3 in Feeney et al, 2019. Guidance for parameter selection comes from the CAESAR-Lisflood website (*Caesar-Lisflood*, 2019)

Figure 4

Map of the goodness of fit area matching results

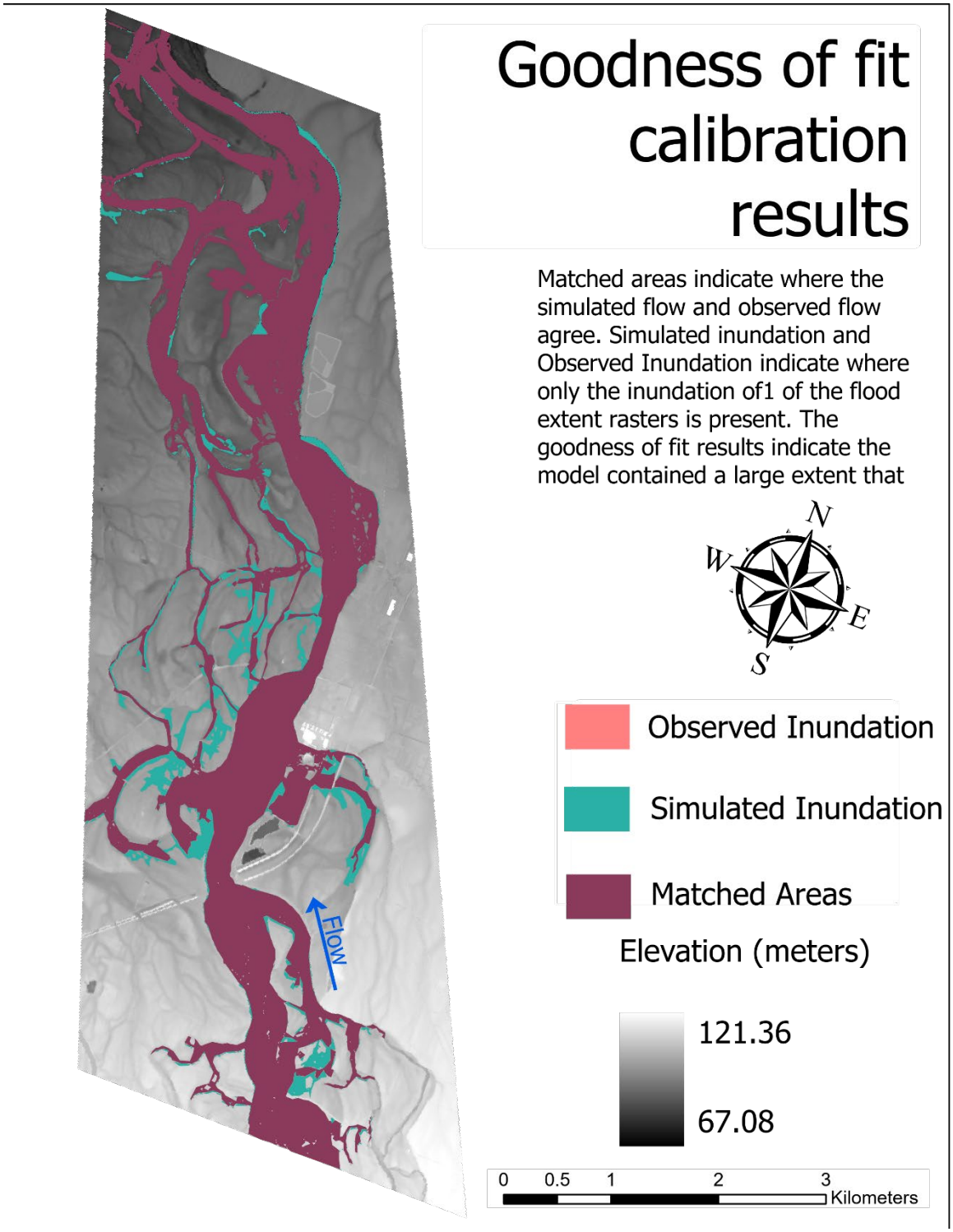

Previous papers noted initial model sediment yields contain exaggerated values due to the model adjusting the terrain to match flow mechanics and winnow fine sediments (Batz, 2010; Meadows, 2014; Feeney, 2020). A model "spin-up" period adjusts the channel for exaggerated initial sediment yields, spatial distribution, and to smooth out the bathymetric artifacts from interpolating the DEM bathymetry (Figure 5). Following Feeney et al. (2020), an annual oscillation between the functional flow and a low flow to create a ten-year synthetic hydrograph. The functional flow as the initial discharge, the discharge lowers to the post-dam mean low flow on the 182_{nd} day before climbing back up to the functional flow discharge on Day 365. This quadratic hydrograph repeats consecutively for a 10-year simulation with only in-channel lateral erosion and sediment recirculation active. Interannual sediment yield variability appears to stabilize at Year 6 which is comparable to previous studies (Figure 7). Moving forward, the 6-year elevation output raster and grain distribution files serve as the initial terrain and grain data for the 1996 and 2014 simulations.

Figure 5

Manipulation of digital elevation data to fill in missing data gaps

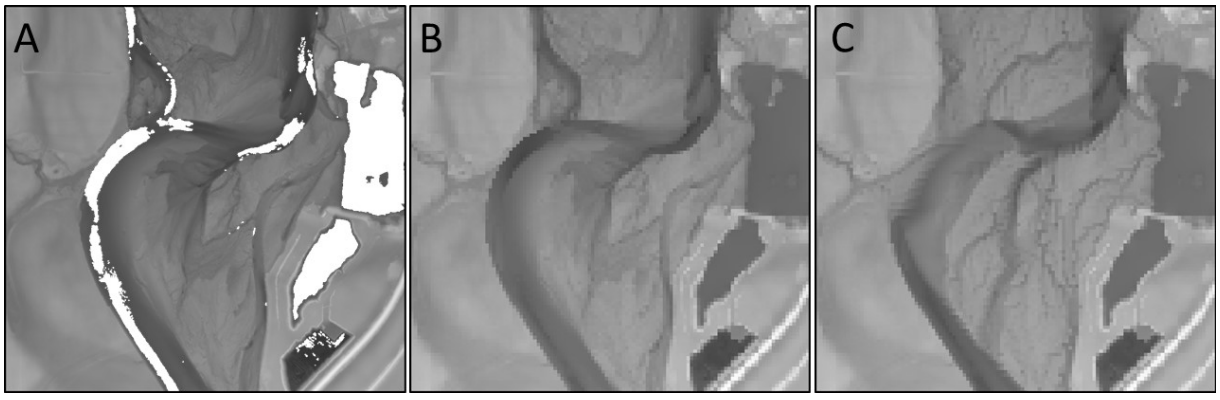

Note. (A) The initial 1-meter resolution topobathymetric lidar DEM with missing bathymetric data. (B) The DEM with holes filled in using sonar and interpolation techniques. (C) Seven year spin-up DEM used for initial simulation conditions.

Figure 6

Spin-up hydrograph showing the oscillating annual peak flow values

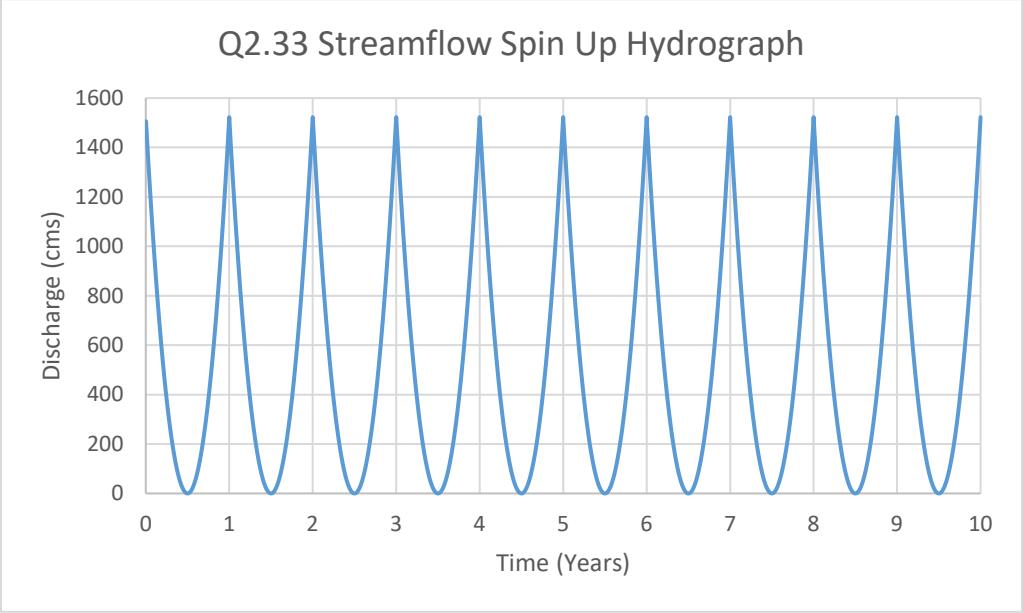

Figure 7

Cumulative Sediment yield results from model spin-up

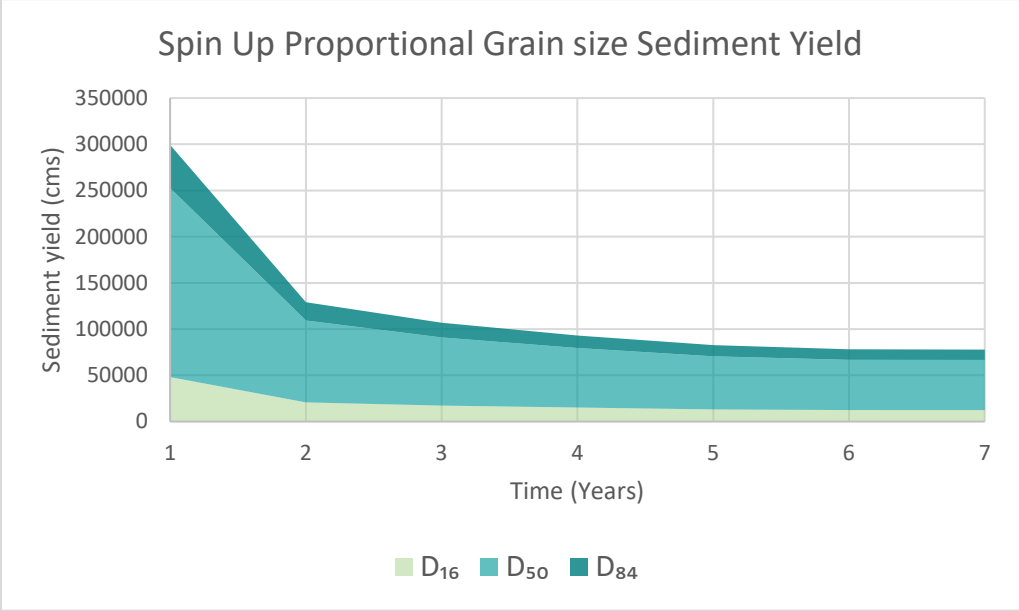

*Note***.** The diagram represents grain size classes individually in this stacked graph to show apportionment and sum. Initial sediment output winnows down to a stable value.

CHAPTER IV

RESULTS

The flood extent for the 1996 event simulation displays an 8.76 km^2 extent with lateral surface water connectivity within the floodplain and inundation of swales and other landforms (Figure 8). The functional flow extent displays an area coverage of 5.56 km^2 including less coverage of bars and landform features within the floodplain. One noticeable difference between the two outputs is the inclusion of more shallow water depth pixels in the 1996 simulation. The functional floodplain simulation shows a fair amount of water depth values exceeding one meter around most secondary feature water edges indicating channels with near vertical banks (entrenched) at this discharge. An analysis of flood extent per discharge iteration shows a high level of correlation for the rising hydrograph limb for both the 1996 and functional flow meaning there is no significant connectivity thresholds above the main channel bankfull level (Figure 9).

Figure 8

Water depth maps for the peak flood extent of the 1996 simulation & functional flow simulation

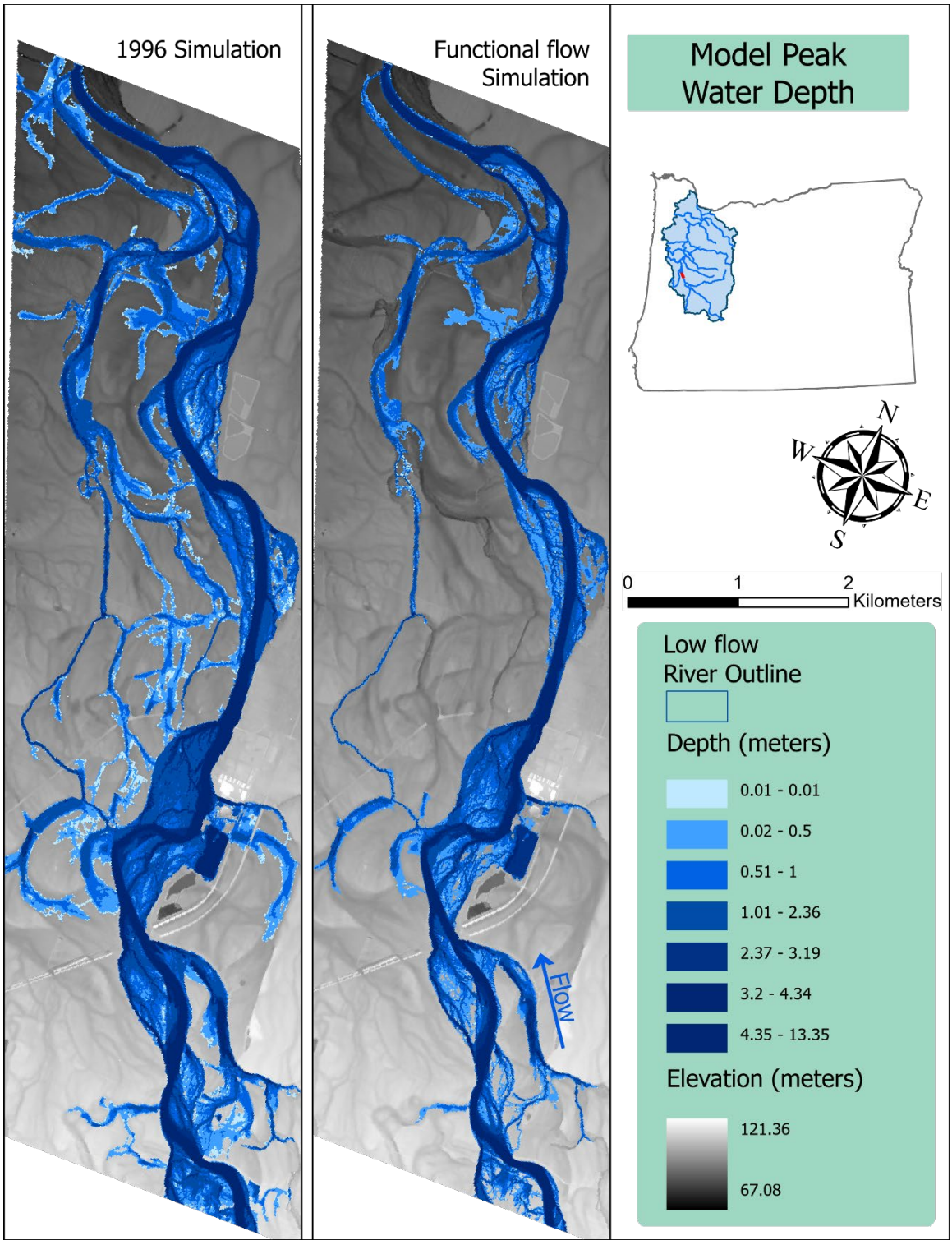

Figure 9

Graphs displaying the changes in flood extent and discharge throughout the rising discharge limb of the hydrograph

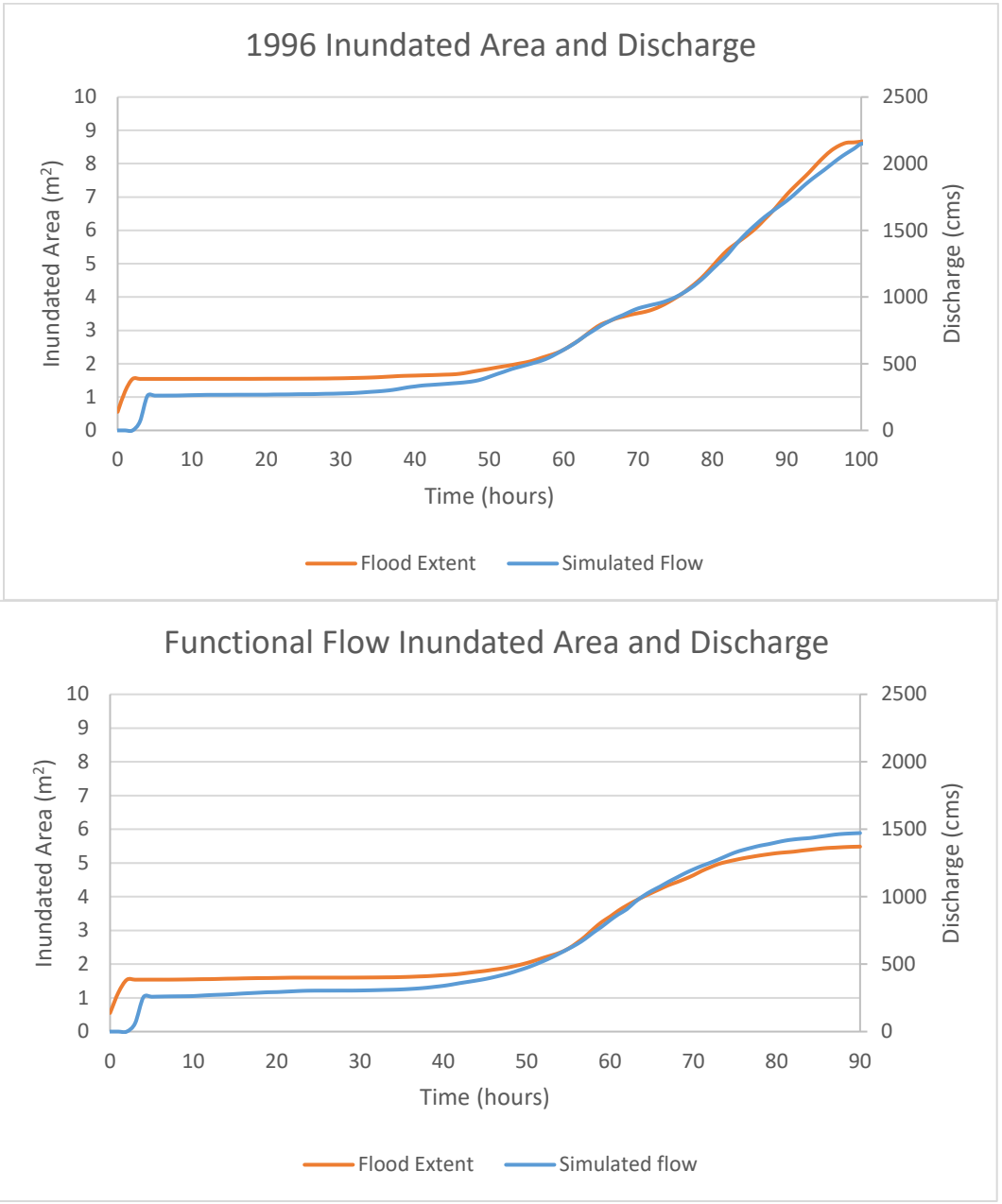

Note. The graphs show (A) 1996 simulation results and (B) Functional flow simulation results.

Erosion and deposition, represented by changes in elevation, range between -2.3 meters and 3.1 meters (Figure 10). Pixels with large magnitude values indicate more elevation change. The area of large erosion and deposition is predominately in-channel for the functional floodplain simulation. The bars show primarily accretion/deposition levels below 0.2 meters on channel bars for the functional floodplain simulation and little change outside of entrenched secondary channels. The 1996 flood also has most of its erosion/deposition within the main channel, but it does more geomorphic change within the floodplain than the functional flow. The floodplain also contains a mixture of higher magnitude erosion and deposition on bars and landforms compared to a more uniform pattern on bars and landforms in the functional flow simulation.

Sediment yield analysis indicates the 1996 flow produced 13,374 cubic meters for the 623-hour simulation while the functional flow produced 6,549 cubic meters of sediment for a 551-hour simulation. This corresponds with the sediment yield graphs showing lower overall yield rates for the functional flow (Figure 11). The 1996 simulation produced a large spike in sediment yield that aligns with the rising limb of the hydrograph, while periods of decreasing flow produced large decreases in sediment yield. The functional flow produced a sediment yield trend that also follows the hydrograph well but includes more noise in temporal variability of sediment yield rate despite having a less variable hydrograph than the 1996 simulation.

Figure 10

Geomorphic change maps produced from the 1996 & functional flow simulations

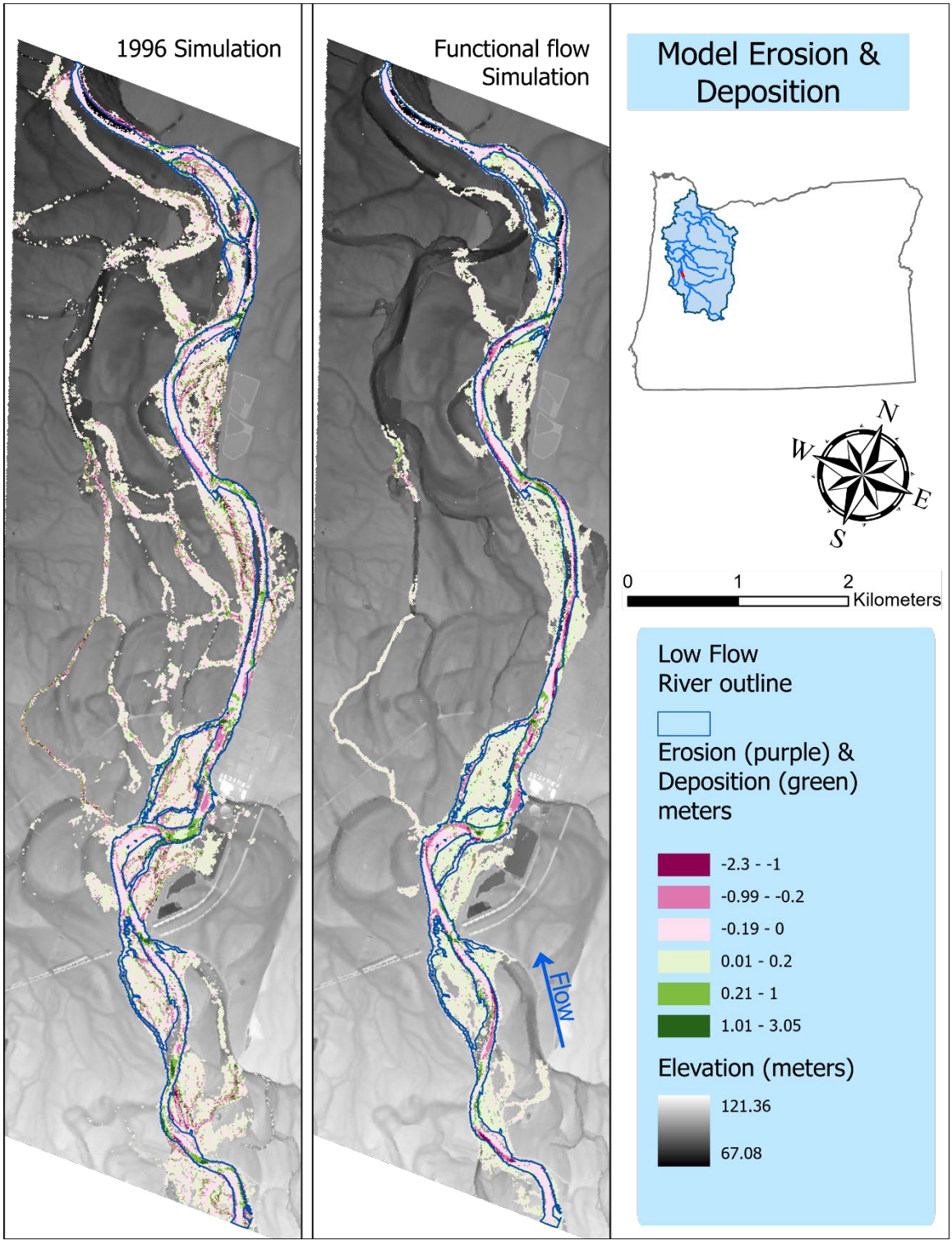

Note. Pixel values represent the total elevation change per pixel.

Figure 11

Sediment yield graphs for the 1996 and Functional flow simulations

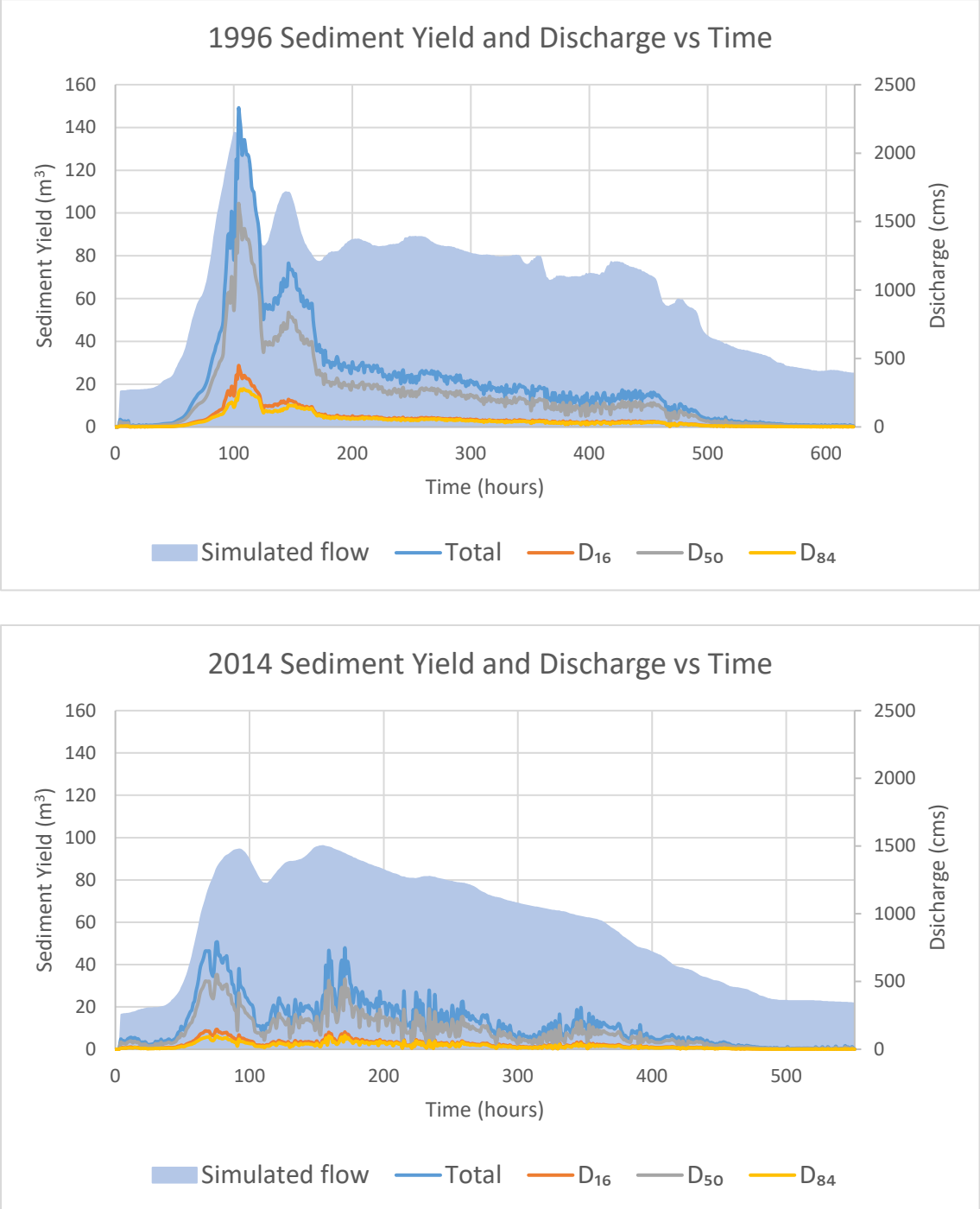

Note. Simulated flow represents the hydrograph. The lines represent the three grain size classes and the overall sediment yield (total).

Table 3

Peak flood extent and total sediment yield for simulations

Simulation	Maximum flood extent	Total Sediment Yield	Simulation Duration
1996 Peak flood event	8.76 km^2	13,374 m^3	623 hours
Functional flow	5.56 km^2	6,549 m^3	551 hours

CHAPTER V

DISCUSSION

Functional Floodplain

The functional floodplain indicates some surface water connectivity between the main channel and floodplain area, but geomorphic activity is confined to primarily the main channel and bars. The inundated areas within the floodplain are predominately in secondary channels and sloughs, with little overbank flooding and connectivity with the floodplain surface. While fish passage data is required to fully assess habitat requirements during flood events, the lack of flood extent and connectivity during the functional flow caused by regulated low discharges and channel modifications raises concerns for suitable low velocity areas for fish during high flow events. Juvenile salmonids rely on secondary water features within the floodplain for increased nutrient-rich habitat as well as refuge from high velocity flows often found during floods (Schroeder et al., 2012). The secondary features inundated by the functional flow contained large stretches with near vertical banks which may not provide refuge from velocities associated with high flow events. The majority of geomorphic change associated with the functional flow occurs in the main channel and bars but there are areas of geomorphic change within the secondary channels where channels are narrow and an increase in channel slope contribute to erosion/deposition (Figure 10).

The 1996 event simulation results indicate an increased inundation of secondary water features and high amounts of surface water connectivity and geomorphic change within the western floodplain. Compared to the functional flow event, the geomorphic patterns along bars showed a more sporadic distribution of erosion and deposition of

varying magnitudes which is favorable to tree stand initiation. As expected, the larger flow showed more inundation and geomorphic change.

In comparison to the 2-year regulated flow bathtub model produced by River Design Group, there is much, much less flood extent in the CAESAR-Lisflood model produced in this study (River Design Group Inc., 2012a). As noted earlier, this bathtub model does not represent connectivity but a projected water surface elevation regardless of flow mechanics, channel connectivity, and hydrology aside from the river stage. The CAESAR-Lisflood modeled flood extents for both the functional flow and the 1996 flood simulations were smaller than the River Design Group bathtub model despite the 1996 flood containing a higher peak discharge at 2,149 cfs compared to the River Design Group two year 1,699 cfs (River Design Group, 2012b). While the bathtub model may represent disconnected pluvial features formed by rising groundwater levels, it is less indicative of peak flow refuge since it does not indicate accurate potential fish passage corridors. Furthermore, the bathtub method only provides results that lean towards engineered static habitats as restoration, as described by Beechie et al. (2010), since geomorphic processes are not included. Using CAESAR-Lisflood provided an image of current lateral connectivity and the inclusion of geomorphic processes for a more holistic approach to evaluating river restoration. For this reason, I believe the use of reach scale hydrodynamic LEMs should be explored in the analysis and evaluation of future restoration projects.

Sediment Transport

The large in-channel erosion values show that most of the geomorphic change associated with the functional flow resides within the channel, little to no change occurs on the floodplain outside of bars and the channelized entrenched sections of secondary channels for the functional floodplain. There is little bedload movement outside of the bars and entrenched secondary channels. Concerning tree stand initiation, the functional flow would contain both erosion and deposition but primary deposition on bars is in a random distribution pattern.

Defining the Functional Flow

Definitions and methodological choices for defining the functional flow impacted the model outcome in multiple ways. The inclusion or exclusion of flood frequency analysis data can determine the discharge of a certain recurrence interval, as presented in Table 1. The introduction of regulated flows manipulates flood frequency analysis in a manner that warrants further critiques for the use of recurrence intervals as representative indicators of thresholds for geomorphic change within a highly modified river system. Furthermore, flow regulation and restoration efforts that accommodate stakeholders construct a moving target for what should be considered the functional floodplain and the corresponding flows. The use of the annual flow as the definition of functional flow represents the regulated flow trend, and it is a better indication for what has occurred and would likely occur moving forward instead of incorporating recurrence intervals associated with geomorphic thresholds on non-regulated rivers. Ultimately, the choice of how the functional flow is defined is determined by the investigator and stakeholders.

Flood frequency analysis choice also played a key role in determining the functional flow. Using the Log-normal statistical fitting method produced lower discharge values than previous studies. As mentioned, this method was chosen due to its simplicity but upon closer analysis of previous studies, the Log-Pearson III method was the previous studies' preferred method. Applying different flood frequency analysis methods produced inconsistent values ranging upwards of 100 cms. Moving forward, more research on flood frequency analysis methods should be conducted to determine the best approach.

Model performance

Flow and Flood Extent

Model flow calibration showed a high level of accuracy only hindered by the lack of high-resolution calibration data. CAESAR-Lisflood produced cell inundation values as low as 1cm. This high level of detail was not possible for the classification of inundated areas in the 1996 aerial imagery, hindering optimal model validation. Additionally, only above-ground artifacts such as bridges were removed from the terrain data, consequently, culverts and other water transport corridors are not represented well in CAESAR-Lisflood. This means connectivity could be higher than what is displayed in the simulation results. Further validation data for lower discharges should be included to improve low flow analysis.

Geomorphic Change

The geomorphic performance of the model is uncertain largely due to the temporal span of the simulated events and the lack of sediment transport data in this area.

Landscape evolution models typically run simulations to represent changes spanning multiple years to multiple decades that are later compared to previous records of channel change as an affirmation of reasonable geomorphic parameters. While geomorphic change can occur rapidly, the magnitude of the modeled events is not necessarily impactful enough to cause comparable amounts of geomorphic change to the channel planform. Furthermore, without observational data for comparison, determining whether the issues are caused by oversimplification of flow dynamics or incorrect parameterization becomes a challenge.

The mean ensemble approach produced mixed results that require further analysis of long-term channel change through potential hindcasting and bedload grain size validation. All hydrograph discharge values simulated were able to transport every grain size and required the creation of the bedrock layer. The bedrock layer prevents the formation high erosion areas caused by potential subcritical flow resulting from model spin-up adjustments. The redistribution of sediment caused by model spin-up also produced large amounts of sediment that redistributed within the channel, and these do not represent likely values. Regardless of the magnitude, the spatial trends classifying erosion and deposition seem to be valid.

Future Research

Further research is needed in the development of lateral connectivity metrics. Unsuccessful attempts were made to develop a precise and discrete connectivity metric, but due to the smooth expansion and coalescence of secondary water features with stage increases, inundation extent served as a good proxy for connectivity.

Moving forward, this model should be tested using updated NAIP imagery of channel change as well as the inclusion of field surveys for more comprehensive grain size data. As more time passes, more channel change occurs, producing a detailed dataset for the evaluation and calibration of model performance. With further development, CAESAR-Lisflood can simulate channel evolution scenarios ranging from larger peak flows to decadal changes using proposed environmental flows. Additionally, the analysis of simulations with stable discharge can help produce more accurate inundation extents to improve the determination of goal-oriented environmental flows.

CHAPTER VI

CONCLUSION

The Willamette River has historically lost channel complexity due to the anthropogenic impacts of dams, bank stabilization, and removal of large woody debris. The simplification of the river planform has also hindered ecosystem dynamics and raised interest in river restoration. This thesis attempts to answer what is the extent of the contemporary functional floodplain of the Willamette River and how well the CAESAR-Lisflood model perform in simulating hydraulic and geomorphic processes of the Willamette River. Simulating the 1996 peak flow produced acceptable flood extent performance, but erosion/deposition values are uncertain due to the lack of validation data. The functional floodplain contained entrenched water features with the majority of the geomorphic change occurring in the channel and bars. Compared to the functional floodplain the 1996 simulation displayed increased flood extent and floodplain connectivity, and geomorphic change. When compared with previous representations of the potential restoration 2-year floodplain, both simulations contained less flood extent due to CAESAR-Lisflood's more sophisticated representation of flow mechanics. With the inclusion of hydrodynamic LEMs, potential environmental flows can be simulated to evaluate functional floodplains as well as improve restoration project design by incorporating geomorphic processes.

REFERENCES CITED

Aikens, C. M. (1975). Archaeological Studies in the Willamette Valley, Oregon (SHPO, 525 Trade Street SE, Salem, or 97310 [0000867]). Department of Anthropology.

Bates, P. D., Horritt, M. S., & Fewtrell, T. J. (2010). A simple inertial formulation of the shallow water equations for efficient two-dimensional flood inundation modelling. Journal of Hydrology, 387(1), 33–45. https://doi.org/10.1016/j.jhydrol.2010.03.027

Batz N. 2010. Predicting ecological diversity of floodplains using a hydromorphic model(CAESAR). accessed date December 17, 2019. Available at: http://edepot.wur.nl/165143.

Beechie, T. J., Sear, D. A., Olden, J. D., Pess, G. R., Buffington, J. M., Moir, H., Roni, P., & Pollock, M. M. (2010). Process-based Principles for Restoring River Ecosystems. BioScience, 60(3), 209–222. https://doi.org/10.1525/bio.2010.60.3.7

Caesar-lisflood. (2019, July 8). SourceForge. Retrieved May 27, 2021, from https://sourceforge.net/projects/caesar-lisflood/

Coulthard, T. J., Hicks, D. M., & Van De Wiel, M. J. (2007). Cellular modelling of river catchments and reaches: Advantages, limitations and prospects. Geomorphology, 90(3–4), 192–207.

Coulthard, T. J., Neal, J. C., Bates, P. D., Ramirez, J., de Almeida, G. A., & Hancock, G. R. (2013). Integrating the LISFLOOD-FP 2D hydrodynamic model with the CAESAR model: Implications for modelling landscape evolution. Earth Surface Processes and Landforms, 38(15), 1897–1906.

Coulthard, T. J., & Van De Wiel, M. J. (2006). A cellular model of river meandering. Earth Surface Processes and Landforms: The Journal of the British Geomorphological Research Group, 31(1), 123–132.

Coulthard, T. J., & Van De Wiel, M. J. (2017). Modelling long term basin scale sediment connectivity, driven by spatial land use changes. Geomorphology, 277, 265–281.

Escobar-Arias, M. I., & Pasternack, G. B. (2010). A hydrogeomorphic dynamics approach to assess in-stream ecological functionality using the functional flows model, part 1—Model characteristics. River Research and Applications, 26(9), 1103–1128. https://doi.org/10.1002/rra.1316

Feeney, C. J., Chiverrell, R. C., Smith, H. G., Hooke, J. M., & Cooper, J. R. (2020). Modelling the decadal dynamics of reach-scale river channel evolution and floodplain turnover in CAESAR-Lisflood. Earth Surface Processes and Landforms, 45(5), 1273–1291. https://doi.org/10.1002/esp.4804

Fierke, M. K., & Kauffman, J. B. (2006). Invasive species influence riparian plant diversity along a successional gradient, Willamette River, Oregon. Natural Areas Journal, 26(4), 376–382.

Graf, W. L. (2006). Downstream hydrologic and geomorphic effects of large dams on American rivers. Geomorphology, 79(3), 336–360. https://doi.org/10.1016/j.geomorph.2006.06.022

Gregory SV Ashkenas LR Oetter D Minear P Wildman K . 2002. Historical Willamette River channel change. Pages. 18-25. in Hulse D Gregory S Baker J, eds. Willamette River Basin Atlas: Trajectories of Environmental and Ecological Change. Corvallis: Oregon State University Press.

Gregory, S. V., Ashkenas, L., & Nygaard, C. (2007). Summary report to assist development of ecosystem flow recommendations for the Coast Fork and Middle Fork of the Willamette River, Oregon.

Gregory, S., Wildman, R., Hulse, D., Ashkenas, L., & Boyer, K. (2019). Historical changes in hydrology, geomorphology, and floodplain vegetation of the Willamette River, Oregon. River Research and Applications, 35(8), 1279–1290. https://doi.org/10.1002/rra.3495

Hayes, D. S., Brändle, J. M., Seliger, C., Zeiringer, B., Ferreira, T., & Schmutz, S. (2018). Advancing towards functional environmental flows for temperate floodplain rivers. Science of The Total Environment, 633, 1089–1104. https://doi.org/10.1016/j.scitotenv.2018.03.221

Johannessen, C. L., Davenport, W. A., Millet, A., & McWilliams, S. (1971). The Vegetation of the Willamette Valley. Annals of the Association of American Geographers, 61(2), 286–302.

King, J., Brown, C., & Sabet, H. (2003). A Scenario-Based Holistic Approach to Environmental Flow Assessments for Rivers. River Research and Applications, 19, 619–639. https://doi.org/10.1002/rra.709

Klingeman, P. C. (1987). Geomorphic influences on sediment transport in the Willamette River. IAHS-AISH Publication, 165, 365–374.

Langston, T. (2015). Spatial Patterns of Sediment Transport in the Upper Willamette River, Oregon.

Leopold, L. B. (1994). A View of the River. Harvard University Press.

Lytle, D. A., & Poff, N. L. (2004). Adaptation to natural flow regimes. Trends in Ecology & Evolution, 19(2), 94–100. https://doi.org/10.1016/j.tree.2003.10.002

Meadows, T. (2014). Forecasting long-term sediment yield from the upper North Fork Toutle River, Mount St. Helens, USA [PhD Thesis]. University of Nottingham.

O'Connor, J. E., Mangano, J. F., Anderson, S. W., Wallick, J. R., Jones, K. L., & Keith, M. K. (2014). Geologic and physiographic controls on bed-material yield, transport, and channel morphology for alluvial and bedrock rivers, western Oregon. GSA Bulletin, 126(3–4), 377–397. https://doi.org/10.1130/B30831.1

Opperman, J., Luster, R., McKenney, B., Roberts, M., & Meadows, A. (2010). Ecologically Functional Floodplains: Connectivity, Flow Regime, and Scale1. JAWRA Journal of the American Water Resources Association, 46, 211–226. https://doi.org/10.1111/j.1752-1688.2010.00426.x

Oregon State Planning Board, 1938. Present and potential land development in Oregon through flood control, drainage and irrigation, Oregon State Planning Board.

Quantum Spatial Inc. (2017) Willamette River, Oregon Topobathymetric LiDAR

Risley, J., Wallick, Jr., Waite, I., & Stonewall, A. (2010). Development of an environmental flow framework for the McKenzie River basin, Oregon.

Risley, J.C., Wallick, J.R., Mangano, J.F., and Jones, K.F., 2012, An environmental streamflow assessment for the Santiam River basin, Oregon: U.S. Geological Survey Open-File Report 2012-1133, 66 p.

River Design Group Inc. (2012a). Willamette River Inundation for 2 year regulated flow [Map].

River Design Group Inc. (2012b). Willamette River Floodplain Inundation Mapping—Eugene to Oregon City. https://oregonexplorer.info/places/basins/willamette?qt-basin_quicktab=1

Schroeder, K., Cannon, B., Whitman, L., & Olmsted, P. (2012). Willamette Spring Chinook: Life in the River. Oregon Department of Fish and Wildlife. https://odfw.forestry.oregonstate.edu/willamettesalmonidrme/sites/default/files/other/2012_chinook_project_handout.pdf

Sedell, J.R. and Froggatt, J.L. (1984) Importance of streamside forests to large rivers: The isolation of the Willamette River, Oregon, USA, from its fl oodplain by snagging and streamside forest removal, Internationale Veriningung fur Theoretische and Angewandte Limnologie Verhandlungen (International Association for Theoretical and Applied Limnology) 22, 1828–1834.

USACE, 1969a. Willamette Basin Comprehensive Study, Appendix E Flood Control, Willamette Basin Task Force-Pacific Northwest River Basins Commission.

USGS. Peak streamflow for Willamette River at Harrisburg. Retrieved December 30, 2020, from http://nwis.waterdata.usgs.gov/usa/nwis/peak/?site_no=14166000

Wallick, J. R. (2004). Geology, flooding & human activities: Establishing a hierarchy of influence for controls on historic channel change, Willamette River, Oregon. https://agris.fao.org/agris-search/search.do?recordID=AV2012048624

Wallick, J. R., Grant, G. E., Lancaster, S. T., Bolte, J. P., & Denlinger, R. P. (2007). Patterns and controls on historical channel change in the Willamette River, Oregon, USA. Large Rivers: Geomorphology and Management, Edited by: Gupta, A., John Wiley & Sons Ltd, 491–516.

Wallick, J.R., Jones, K.L. O'Connor, J.E., Keith, M.K., Hulse, David, and Gregory, S.V., 2013, Geomorphic and vegetation processes of the Willamette River floodplain, Oregon—Current understanding and unanswered questions: U.S. Geological Survey Open-File Report 2013-1246., 70 p., http://dx.doi.org/10.3133/ofr20131246.

Ward, J. V. (1989). The Four-Dimensional Nature of Lotic Ecosystems. Journal of the North American Benthological Society, 8(1), 2–8. https://doi.org/10.2307/1467397

White, J.S., Gordon, G.W., and Overstreet, B.T., 2019, Single-beam Echosounder Bathymetry of the Willamette River, Oregon 2015-2018: U.S. Geological Survey data release, https://doi.org/10.5066/P92TTY4R.

Wilcock, P. R., & Crowe, J. C. (2003). A surface-based transport model for sand and gravel. Hydraulic Engineering, 129(2), 120.

Williams, G. P. (1978). Bank-full discharge of rivers. Water Resources Research, 14(6), 1141–1154.

Wohl, E. (2017). Connectivity in rivers. Progress in Physical Geography, 41(3), 345–362.

Yarnell, S. M., Petts, G. E., Schmidt, J. C., Whipple, A. A., Beller, E. E., Dahm, C. N., Goodwin, P., & Viers, J. H. (2015). Functional Flows in Modified Riverscapes: Hydrographs, Habitats and Opportunities. BioScience, 65(10), 963–972. https://doi.org/10.1093/biosci/biv102

Zeug, S. C., & Winemiller, K. O. (2008). Relationships between hydrology, spatial heterogeneity, and fish recruitment dynamics in a temperate floodplain river. River Research and Applications, 24(1), 90–102. https://doi.org/10.1002/rra.1061